

X Nuclear Applications on the 21.1 T Magnet at the National High Magnetic Field Laboratory

Jens Rosenberg, Samuel C. Grant, William Brey
 The National High Magnetic Field Laboratory, Florida State University, Tallahassee
 Thomas Oerther, Bruker BioSpin GmbH, Rheinstetten, Germany

The 21.1 T magnet

The 21.1-T, 900 -MHz magnet is a one-of-a-kind magnet. The 105-mm diameter bore accommodates room temperature shims, imaging gradients, RF coils, animal support/monitoring apparatus and *in vivo* specimens up to 350-gr. It is currently equipped with a four channel Bruker Avance® III spectrometer capable of magnetic resonance imaging (MRI), micro imaging and NMR spectroscopy using ParaVision and TopSpin. The superconducting magnet was designed and built entirely at the National High Magnetic Field Laboratory (NHMFL), made possible by a \$16 million grant from the National Science

Foundation (NSF) (1). For imaging, both RRI and Bruker imaging gradient sets are available. Most RF coils are homebuilt by the NHMFL and its users (2,3).

Since the magnet was commissioned in 2005, it has now generated over 100 publications in a wide array of applications for MRI and NMR. This application letter will cover some of the most recent and notable work in MRI that highlight the benefit of ultra-high magnetic fields.

Figure 1

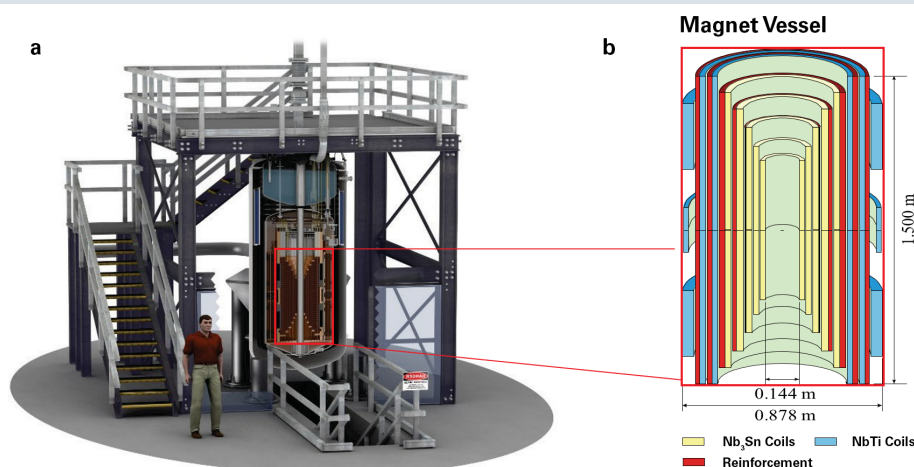


Figure 1a: Illustration of 21.1-T magnet with magnet vessel, support structure, cryostat and cryogenics.

Figure 1b: illustrates the magnet vessel with Nb₃Sn (yellow) and NbTi (blue) coils.

Sodium MRI at 21.1 T

Ultra-high field imaging has proven particularly beneficial for X-nuclei imaging, such as ^{23}Na MRI for which a change in B_0 from 9.4 to 21.1 T resulted in an SNR gain of ~ 3 compared to a gain of ~ 2 for ^1H MR (4). As such, comparable SNR achieved with 36 averages at 21.1 T requiring approximately 100 averages at 9.4 T and greater than 300 averages at 3 T if similar ^{23}Na MRI acquisition protocols are utilized (5-8).

Sodium signal-based enhancements have enabled studies of stroke and migraine in preclinical models. Sodium, potentially a valuable biomarker, is an important indicator of tissue viability and integrity. Differential intracellular versus extracellular sodium distributions may probe cellular function related to ionic homeostasis and $\text{Na}^+/\text{K}^+-\text{ATPase}$ transport. We have demonstrated that, using sodium MRI at ultra-high fields, a significant reduction in stroke lesion size with adult stem cell therapy is observed, while metrics based on ^1H MRI did not change significantly (9,10). In other diseases like migraine, Na^+ instability or dysfunction can manifest as extra- and intracellular changes temporally (11,12). Localized sodium changes have been seen using a slice selective chemical shift imaging (CSI) sequence (13). To better understand the extracellular and intracellular bound sodium, a triple quantum (TQ) ^{23}Na sequence has been developed and compared to an inversion recovery (IR) approach (14). TQ selection, despite sacrifices in temporal resolution compared to IR, provides higher SNR and efficiencies for assessing bound sodium, particularly at low concentrations. Most critically, TQ quantification of *in vivo* bound sodium concentrations were demonstrated to be much more accurate than the IR approach in terms of percent error and absolute quantification

Fluorine MRI at 21.1 T and comparison with 9.4 T

Of course, increased sensitivity at higher fields benefits other X nuclei besides ^{23}Na . Fluorine (^{19}F), even though a $1/2$ spin, provides sensitivity gains with high field MRI. The ^{19}F probes lack endogenous signals in living organisms hence ^{19}F labeled cells *in vivo* can be detected with complete signal selectivity and specificity. This feature is particularly useful in studies using ^{19}F nanoparticles to follow inflammatory cells into target organs such as the brain. However, the detection can be hampered by limited amounts of inflammatory cells, the amount of ^{19}F atoms taken up by the cells and the low signal sensitivity of commercially available MR equipment. One way to improve signal sensitivity is through higher magnetic fields (B_0), for which intrinsic sensitivity is expected to grow at least linearly. Recent studies have compared fluoro-15-crown-5-ether (PFCE) both in phantom and *ex vivo* in an animal model of experimental autoimmune encephalomyelitis (EAE) at 9.4 and 21.1 T (15). Using similar RF coils and scan parameters, a SNR gain of 2.1 was achieved with PFCE nanoparticles using a spin-echo (SE) sequence. This gain is close to the

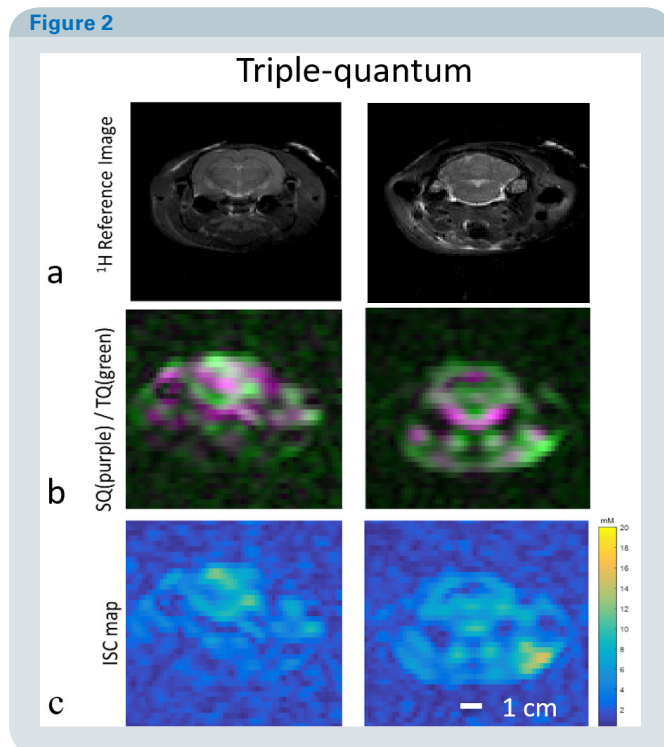


Figure 2: Representative *in vivo* images from two coronal slices through naïve rodent brains (n=2), for ^1H and ^{23}Na acquisitions using TQ and IR acquisitions. **a:** ^1H spin echo for anatomical localization, **b:** ^{23}Na composite tissue sodium concentration (TSC) (purple) and bound sodium concentration (BSC) (green) maps and **c:** BSC maps. 3D TQ images acquired in 20 min, demonstrate excellent filtering of free sodium signal predominantly from ventricular areas and eyes as shown by the composite images (b). The nominal resolution of the images is $1\times 1\times 1\text{ mm}^3$ for both sodium-based acquisitions.

simulated electromagnetic field (EMF) which showed a SNR gain of 2.8. Using a fast low angle shot (FLASH) sequence, a slightly higher SNR gain (gain of 3) was achieved but that also was dependent on the flip angle. It also was expected that relaxation time would change when moving to higher fields. Not surprisingly, T_2 of PFCE decreased with increasing field. T_1 also decreased, contrary to water T_1 . This decrease is attributed to dipole-dipole and chemical shift anisotropy (16). Consistent with the SNR gain at 21.1 T, *ex vivo* experiments of EAE mice treated with PFCE nanoparticles show increased SNR and increased detectability at 21.1 T compared to 9.4 T (15).

Figure 3

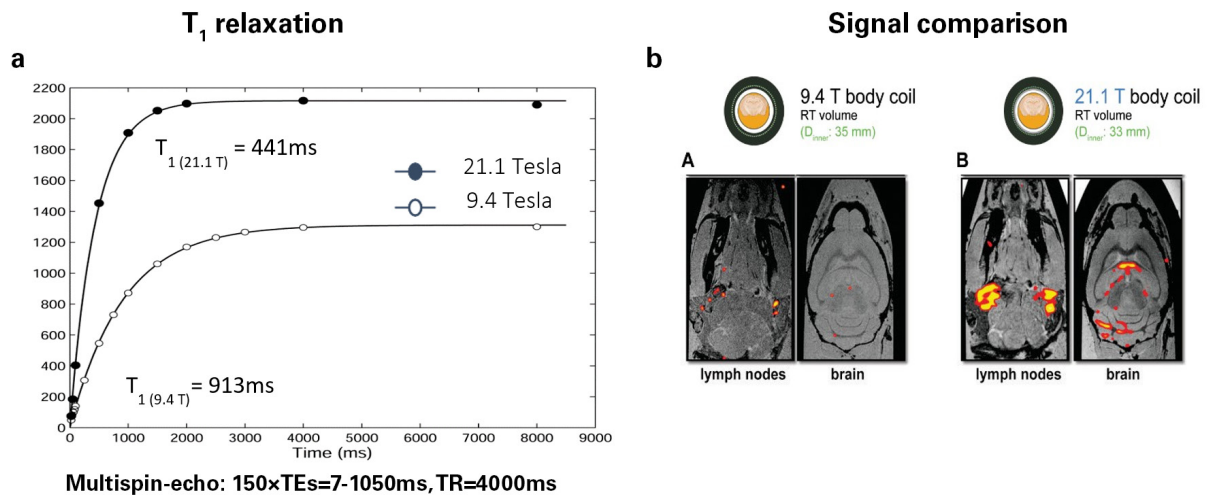


Figure 3a: T₁ relaxation of PFCE particles at 9.4 T vs. 21.1 T. The shorter T₁ is attributed to dipole-dipole and chemical shift anisotropy (16). **Figure 3b:** Here the increased sensitivity of ¹⁹F MRI at 21.1 T is shown with an increase in ¹⁹F signal in the PFCE injected EAE mice. The *ex vivo* sample was scanned with similar coil and scan parameters at both 9.4 and 21.1 T.

Chemical Exchange Saturation Transfer (CEST)

High field CEST benefits from longer T₁ relaxation of water and spectral separation. CEST MRI contrast and quantification benefits from exchangeable protons that are labeled selectively by a limited bandwidth (frequency selective) RF pulse. Following exchange with bulk water protons, this selective saturation decreases the main water signal used for generating neurological MR images. When measured at ultra-high field strength, CEST relaxation mechanisms could open up untapped contrasting possibilities. A recent study explored this potential contrast in two neurological diseases, stroke and brain tumors (17). Fast spin-echo images weighted by

CEST contrast were collected from Sprague-Dawley rats at 21.1 T, focusing on a middle cerebral artery occlusion model emulating ischemic stroke and xenografted glioma cells that were followed over the course of several days as they developed into tumors. An intense CEST contrast as measured by magnetic transfer ratio asymmetry (MTR_{asym}) was observed in rat glioma tissues and considerably larger than that hitherto observed at lower fields. Several processing methods were used to identify and quantify the various contributions to this enhanced MTR_{asym}. By contrast, the changes in MTR_{asym} did not reach statistical significance in the subacute ischemic cases. This study shows that CEST at ultra-high fields could open up new endogenous potential biomarkers for pathology.

Figure 4

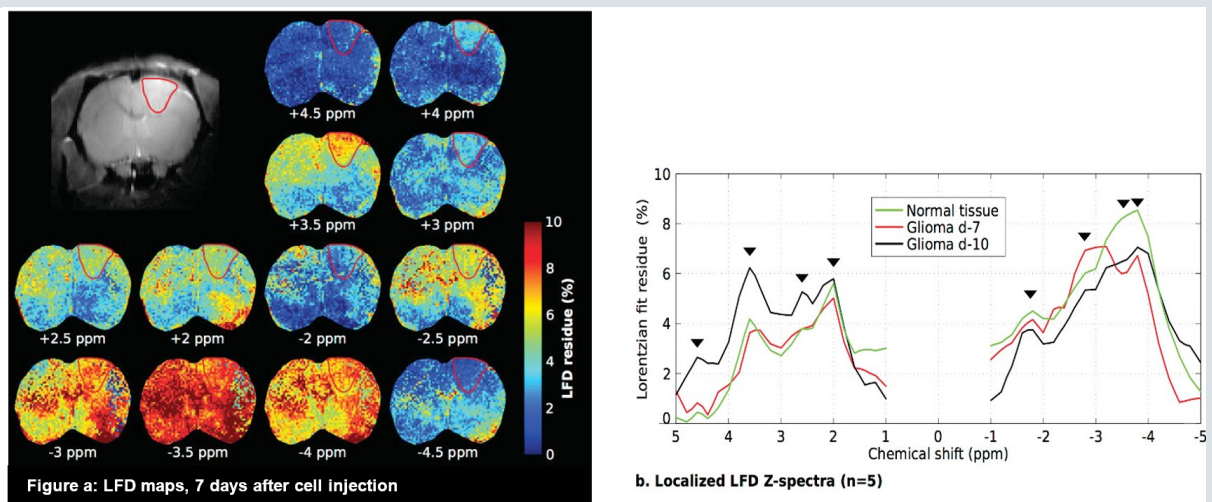


Figure 4a: Quantitative CEST maps obtained using the Lorentzian fit difference (LFD) method on a rat 7 days post tumor implant. Notice the strong positive contrast appearing at +3.5 ppm (APT) and the slight negative contrast observed at -3.5 ppm (NOE) for the tumorous tissue. **Figure 4b:** CEST Z-spectra obtained using LFD. The black arrows indicate multiple spectral features arising with glioma-induced changes as function of days after injection. The vertical scale denotes % with respect to the maximum water signal S₀.

References

- [1] Fu R, Brey WW, Shetty K, et al. Ultra-wide bore 900 MHz high-resolution NMR at the National High Magnetic Field Laboratory. *J Magn Reson* **2005**:177:1-8.
- [2] 2. Qian C, Masad IS, Rosenberg JT, et al. A volume birdcage coil with an adjustable sliding tuner ring for neuroimaging in high field vertical magnets: Ex and in vivo applications at 21.1 T. *J Magn Reson* **2012**:221:110-116.
- [3] 3. Rosenberg JT, Shemesh N, Muniz JA, Dumez JN, Frydman L & Grant SC. Transverse relaxation of selectively excited metabolites in stroke at 21.1 T. *Magn Reson Med* **2016**.
- [4] 4. Schepkin VD, Brey WW, Gor'kov PL & Grant SC. Initial in vivo rodent sodium and proton MR imaging at 21.1 T. *Magn Reson Imaging* **2010**:28:400-407.
- [5] 5. Wetterling F, Ansar S & Handwerker E. Sodium-23 magnetic resonance imaging during and after transient cerebral ischemia: multinuclear stroke protocols for double-tuned (23)Na/(1)H resonator systems. *Phys Med Biol* **2012**:57:6929.
- [6] 6. Lin SP, Song SK, Miller JP, Ackerman JJ & Neil JJ. Direct, longitudinal comparison of (1)H and (23)Na MRI after transient focal cerebral ischemia. *Stroke* **2001**:32:925-932.
- [7] 7. Thulborn KR, Gindin TS, Davis D & Erb P. Comprehensive MR imaging protocol for stroke management: tissue sodium concentration as a measure of tissue viability in nonhuman primate studies and in clinical studies. *Radiology* **1999**:213:156-166.
- [8] 8. Wetterling F, Gallagher L, Mullin J, et al. Sodium-23 magnetic resonance imaging has potential for improving penumbra detection but not for estimating stroke onset time. *J Cereb Blood Flow Metab* **2015**:35:103-110.
- [9] 9. Rosenberg JT, Sellgren KL, Sachi-Kocher A, et al. Magnetic resonance contrast and biological effects of intracellular superparamagnetic iron oxides on human mesenchymal stem cells with long-term culture and hypoxic exposure. *Cytotherapy* **2013**:15:307-322.
- [10] 10. Rosenberg JT, Sellgren K, Calixto-Bejarano F, et al. MR Contrast and Biological Impacts of Intracellular Superparamagnetic Iron Oxides on Human Mesenchymal Stem Cells with Hypoxic Ischemic Exposure. *Proc. Intl. Soc. Mag. Reson. Med.* **2012**:4365.
- [11] 11. Harrington MG. Cerebrospinal fluid biomarkers in primary headache disorders. *Headache* **2006**:46:1075-1087.
- [12] 12. Harrington MG, Chekmenev EY, Schepkin V, Fonteh AN & Arakaki X. Sodium MRI in a rat migraine model and a NEURON simulation study support a role for sodium in migraine. *Cephalalgia* **2011**:31:1254-1265.
- [13] 13. Abad N, Rosenberg JT, Hike DC, Harrington MG & Grant SC. Dynamic sodium imaging at ultra-high field reveals progression in a preclinical migraine model. *Pain* **2018**:159:2058-2065.
- [14] 14. Abad N, Amouzandeh G, Mentink-Vigier F, Rosenberg J, Harrington M & Grant S. Assessment of Bound Sodium using Triple Quantum Selection vs. Inversion Recovery at 21.1 T: A Phantom and in vivo Rodent Study of Naïve, Ischemic and Hydrocephalic Conditions. *NMR Biomedicine* **2019**.
- [15] 15. Waiczies S, Rosenberg JT, Kuehne A, et al. Fluorine-19 MRI at 21.1 T: enhanced spin-lattice relaxation of perfluoro-15-crown-5-ether and sensitivity as demonstrated in ex vivo murine neuroinflammation. *MAGMA* **2019**:32:37-49.
- [16] 16. Kadayakkara DK, Damodaran K, Hitchens TK, Bulte JW & Ahrens ET. (19)F spin-lattice relaxation of perfluoropolyethers: Dependence on temperature and magnetic field strength (7.0-14.1T). *J Magn Reson* **2014**:242:18-22.
- [17] 17. Roussel T, Rosenberg JT, Grant SC & Frydman L. Brain investigations of rodent disease models by chemical exchange saturation transfer at 21.1 T. *NMR Biomed* **2018**:31:e3995